

to be constrained⁴. Third, future sexual selection models should acknowledge that a mating bias for indirect-benefits or ‘good genes’ can result in conflicting sex-specific offspring fitness⁴. □

Methods

Organismal maintenance

Crickets were maintained in plastic cages (10 × 10 × 8 cm) containing ground cat food and a carrot slice (provided ad libitum), dampened cheesecloth (water source and oviposition material) and strips of brown paper towel for cover. The food, carrot and paper towel were replaced every two days. Cages were kept in a constant environment at 28 °C and a 12:12 light–dark photoperiod provided by a Percival incubator. The age of laboratory-reared experimental crickets was 10 ± 1 days post-eclosion (final adult moult).

Mating trials

Mating arenas were made from 100-mm Petri dishes lined with filter paper. Males from both successful and unsuccessful sires were randomly chosen for each mating trial to provide an equal sire-group representation. Females were also randomly chosen from either sire group. To help control for the potential influence of mating experience, males were tested against other males who had shared an equal number of previous trials (that is, 0, 1, 2, and so on). Each male was mated once per day. After mating, females were isolated to oviposit until their death. All trials were videotaped.

Statistical analysis

Repeatabilities (*R*) were estimated by calculating the intra-class correlation obtained from a one-way ANOVA (that is, $R = (MS_{\text{among}} - MS_{\text{error}}) / [MS_{\text{among}} + (N - 1)MS_{\text{error}}]$, where *MS* is the mean square estimate and *N* is the number of repeated measures per individual)¹⁴. Genetic correlation coefficients were based on sire family means (*n* = 47). Because correlation estimates were cross-generational (that is, sire–offspring), estimates of trait (co)variance were based on different individuals within each sire family (as opposed to the same individuals), thereby providing a relatively unbiased estimator of the additive genetic correlation. Tests of significance were based on correlation-coefficient critical values derived from standard statistical tables¹⁵.

For each sex, \bar{w} among sire groups was calculated as:

$$\bar{w}_{jg} = \left(\sum_1^{n_g} (w_{ji} / w_{j\text{max}}) \right) / n_{jg} \quad (1)$$

where *w* is the average offspring fitness of sex *j* for the *i*th sire; *w*_{max} represents the maximum observed fitness value; *g* represents the sire group (successful or unsuccessful); and *n* is the number of sires. Thus, four estimates of average relative fitness were calculated including the sons and daughters of successful sires, as well as the sons and daughters of unsuccessful sires. To correct for potential differences in sex ratio between sire groups, we recalculated \bar{w} by first multiplying *w*_{*ji*} by *a*_{*ji*}, where *a* is the offspring abundance of sex *j* for the *i*th sire. Each new male and female estimate of \bar{w} was then divided by their respective population sex ratios (male:female is 0.89 and female:male is 1.12), to adjust for the difference in the fisherian value between the sexes; that is, because fewer males existed, they possessed a higher breeding value. All analyses were performed using SAS v8.

Received 4 February; accepted 9 March 2004; doi:10.1038/nature02492.

1. Kokko, H. Fisherian and ‘good genes’ benefits of mate choice: how (not) to distinguish between them. *Ecol. Lett.* **4**, 322–326 (2001).
2. Boake, C. R. B. Genetic consequences of mate choice: a quantitative genetic method for testing sexual selection theory. *Science* **227**, 1061–1063 (1985).
3. Heisler, I. L. Quantitative genetic models of female choice based on “arbitrary” male characters. *Heredity* **55**, 187–198 (1985).
4. Chippindale, A. K., Gibson, J. R. & Rice, W. R. Negative genetic correlation for adult fitness between sexes reveals ontogenetic conflict in *Drosophila*. *Proc. Natl Acad. Sci. USA* **98**, 1671–1675 (2001).
5. Rice, W. R. Dangerous liaisons. *Proc. Natl Acad. Sci. USA* **97**, 12953–12955 (2000).
6. Chapman, T., Arnqvist, G., Bangham, J. & Rowe, L. Sexual conflict. *Trends Ecol. Evol.* **18**, 41–47 (2003).
7. Fedorka, K. M. & Mousseau, T. A. Tibial spur feeding in ground crickets: larger males contribute larger gifts (Orthoptera: Gryllidae). *Florida Entomol.* **85**, 317–323 (2002).
8. Fedorka, K. M. & Mousseau, T. A. Nuptial gifts and the evolution of male body size. *Evolution* **56**, 590–596 (2002).
9. Wedell, N. & Tregenza, T. Successful fathers sire successful sons. *Evolution* **53**, 620–625 (1999).
10. Mousseau, T. A. & Dingle, H. Maternal effects in insect life histories. *Annu. Rev. Entomol.* **36**, 511–534 (1991).
11. Mousseau, T. A. & Dingle, H. in *The Unity of Evolutionary Biology* (ed. Dudley, E. C.) 745–761 (Dioscorides, Portland, Oregon, 1991).
12. Roff, D. A. *Evolutionary Quantitative Genetics* (Chapman & Hall, New York, 1997).
13. Montalvo, A. M. & Shaw, R. G. Quantitative genetics of sequential life history and juvenile traits in the partially selfing perennial, *Aquilegia caerulea*. *Evolution* **48**, 828–841 (1994).
14. Zar, J. H. *Biostatistical Analysis* 2nd edn, 324 (Prentice Hall, Englewood Cliffs, New Jersey, 1984).
15. Lynch, M. & Walsh, B. *Genetics and Analysis of Quantitative Traits* 632–637 (Sinauer Associates, Sunderland, 1998).

Acknowledgements We thank D. Promislow, P. Mack and J. Burger for comments on previous manuscript versions. We also thank N. Leung and A. Penn for assisting with cricket maintenance and data collection. This work was supported by a NSF Doctoral Dissertation Improvement Grant to K.M.F. and a NSF grant to T.A.M.

Competing interests statement The authors declare that they have no competing financial interests.

Correspondence and requests for materials should be addressed to K.M.F. (fedorka@uga.edu).

.....
Naturalistic experience transforms sensory maps in the adult cortex of caged animals

Daniel B. Polley^{1,*}, Eugen Kvašňák¹ & Ron D. Frostig^{1,2,3}

¹Department of Neurobiology and Behavior, ²Department of Biomedical Engineering and ³The Center for the Neurobiology of Learning and Memory, University of California, Irvine, California 92697-4550, USA

* Present address: Keck Center for Integrative Neuroscience, University of California, San Francisco, 513 Parnassus Avenue, San Francisco, California 94143-0732, USA

Much of what is known about the functional organization and plasticity of adult sensory cortex is derived from animals housed in standard laboratory cages^{1,2}. Here we report that the transfer of adult rats reared in standard laboratory cages to a naturalistic habitat modifies the functional and morphological organization of the facial whisker representation in the somatosensory ‘barrel’ cortex. Cortical whisker representations, visualized with repeated intrinsic signal optical imaging in the same animals, contracted by 46% after four to six weeks of exposure to the naturalistic habitat. Acute, multi-site extracellular recordings demonstrated suppressed evoked neuronal responses and smaller, sharper constituent receptive fields in the upper cortical layers (II/III), but not in the thalamic recipient layer (IV), of rats with naturalistic experience. Morphological plasticity of the layer IV barrel field was observed, but on a substantially smaller scale than the functional plasticity. Thus, transferring animals to an environment that promotes the expression of natural, innate behaviours induces a large-scale functional refinement of cortical sensory maps.

In a previous study, we demonstrated that natural behaviours could have a powerful impact on the expression of plasticity in whisker-deprived adult rats, given a brief opportunity for natural whisker use outside the standard home cage³. We found that a few minutes of natural whisker use per week induces a profound contraction of the remaining (spared) whisker’s cortical representation, and a decrease of its peak amplitude in contrast to the expansion and increase in peak amplitude of the remaining whisker representation that is commonly observed in rats that remain exclusively in their home cage^{3–8}. In this study, we examined whether the effects of natural whisker use are limited to the cortex of whisker-deprived rats, or if similar plasticity can be observed in the barrel cortex of non-deprived adult rats, given greater opportunity for natural whisker use outside the home cage. Rather than simply elevate sensory activity through a traditional ‘enriched environment’ (typically, a larger cage filled with various toys, a running wheel and conspecifics), we used a new type of environment, the naturalistic habitat (NH), which promotes innate sensorimotor behaviours such as subterranean tunnelling, foraging and three-dimensional navigation, in addition to interactions with conspecifics (Supplementary Fig. S1).

We also compared functional plasticity induced through naturalistic experience to potential changes in the anatomical architecture of the cortex. The barrel cortex is uniquely suited to address this question, given the isomorphic representation of each whisker on the snout with an isolated cluster of granular cells in layer IV of the contralateral posteromedial barrel subfield (PMBSF), called a barrel⁹. Although the gross morphology of the layer IV barrel map can be markedly altered, this effect is strictly limited to the first week of postnatal life^{10,11}. The absence of anatomical reorganization in the adult PMBSF seems to be at odds with reports that experience in traditional enriched environments can produce a host of anatomical changes in the adult neocortex¹²⁻¹⁴. This discrepancy may be caused by a difference in methodology; the critical period for barrel field plasticity has been defined from methods that create imbalances in the level of sensory activity through denervation or deafferentation of the whisker pad, whereas anatomical plasticity in enriched

environments is thought to result from enhancing the amount and complexity of sensory activity.

The area and evoked peak amplitude of individual functional whisker representations were measured with chronic intrinsic signal optical imaging (ISI), before and after rats were exposed to the standard cage (SC) or NH. The area and overlap of individual functional whisker representations did not change systematically in the four to six week interval between imaging sessions in SC rats (Fig. 1a-d). In contrast, after four to six weeks of exposure to the NH, functional whisker representations were extensively contracted and less overlapping in NH rats (Fig. 1e-h). A quantitative analysis of functional whisker representations assessed at multiple activity thresholds demonstrated that the average area of a single whisker's functional representation did not differ before assignment to the NH or SC ($F_{1,19} = 0.07$; $P > 0.05$; Fig. 2a). In the second imaging session the area of a single whisker's representation contracted by an average of 46% in NH rats ($F_{1,12} = 14.58$; $P < 0.005$), but did not change significantly for SC rats ($F_{1,7} = 0.12$; $P > 0.05$), yielding a significant interaction between treatment groups and imaging session ($F_{1,19} = 7.22$; $P < 0.05$; Fig. 2b). In addition to the areal contraction, we observed a significant reduction in the whisker-evoked peak amplitude in NH rats ($-19.77 \pm 6.0\%$, $t = 3.01$; $P < 0.05$), but not in SC rats ($-2.07 \pm 4.26\%$, $t = 0.7$; $P > 0.05$; Fig. 2c), between the first and second imaging session. To determine whether the decrease in the area of a single whisker's representation (measured at absolute optical response thresholds) was attributable to a decrease in the overall amplitude of the whisker-evoked response, areal extent measurements were also made after activity levels were normalized to the peak response. The area at half height measured with this approach did not change between the first and second imaging session in SC rats (3.24 ± 0.67 versus 3.17 ± 0.42 mm²), but contracted by 46.3% between the first and second imaging sessions in NH rats (3.2 ± 0.42 versus 1.72 ± 0.31 mm²), demonstrating that a single whisker's representation contracted within the functional whisker map (Fig. 2d). Additional analyses of the ISI data demonstrated that the contraction could not be accounted for by a change in baseline signal

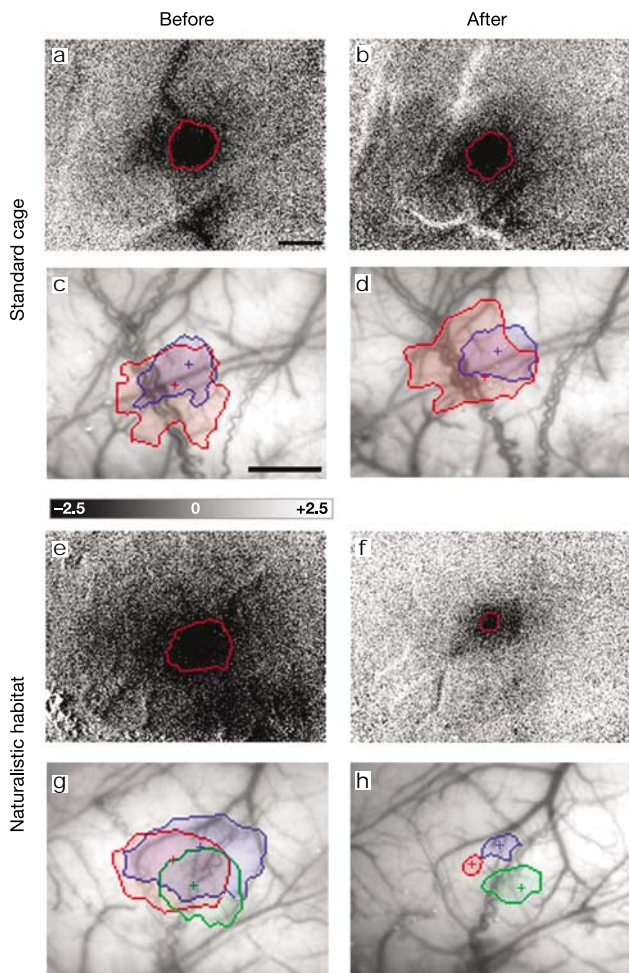


Figure 1 Chronic optical imaging of functional whisker representations through the intact skull. For all panels, Colour boundaries demarcate cortical areas with intrinsic signal activity $\geq 2.5 \times 10^{-4}$. **a, b, e, f**, Ratio images of the C2 whisker representation collected before (**a** and **e**) and after (**b** and **f**) exposure to SC (**a** and **b**) or NH (**e** and **f**). Greyscale bar indicates intrinsic signal strength $\times 10^{-4}$. Black and white streaks correspond to large surface blood vessels. Scale bar in **a**, which also applies to **b, e** and **f**, = 1 mm. **c, d, g, h**, Functional representations for whisker C1 (blue) (red) and B2 (green; in **c** and **h**), obtained from two different SC (**c** and **d**) and NH (**g** and **h**) rats, superimposed onto images of the cortical surface as seen through the thinned skull before (**c** and **g**) and after (**d** and **h**) exposure. Functional peaks for each whisker are indicated by a cross. Scale bar in **c**, which also applies to **d, g** and **h**, = 1 mm.

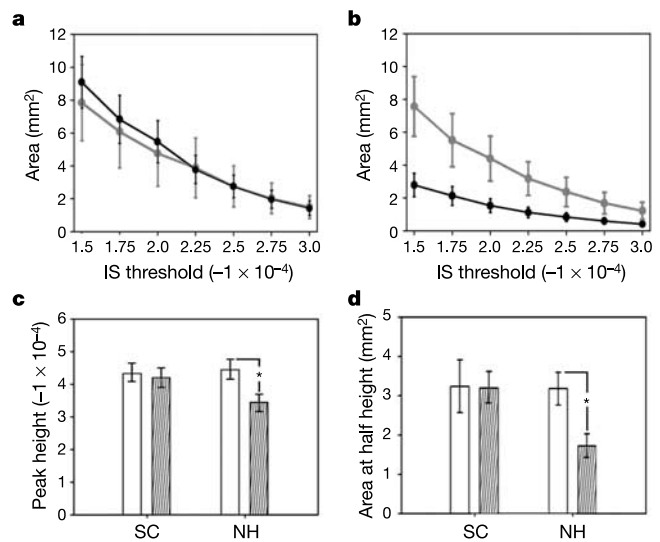


Figure 2 Plasticity of functional whisker representations. **a, b**, Areal extent measured across seven activity thresholds of a single whisker's functional representation, imaged before (**a**) and after (**b**) exposure to NH (black line) and SC (grey line) conditions. IS, intrinsic signal. **c**, Peak height and **d**, area at half height are shown before (open bars) and after (patterned bars) exposure. Asterisks indicate a statistically significant difference ($P < 0.05$) between groups using a paired *t*-test.

strength, or a shift in the temporal profile of the intrinsic signal response (see Supplementary Information). Finally, the contraction of the whisker representation was confirmed by post-imaging single unit recordings (Supplementary Fig. S2).

Next, using simultaneous recordings from an eight-electrode array, we measured receptive field size and whisker-evoked response strength in 349 single and multiunit clusters—located in layer II/III (NH, $n = 90$; SC, $n = 81$) and layer IV (NH, $n = 112$; SC, $n = 66$) from five SC and five NH rats—to determine how the plasticity of cortical population responses observed with ISI corresponded to plasticity in neuronal response properties (Supplementary Fig. S3). Receptive field size measured in layer IV was highly similar in SC and NH rats (median receptive field size is four whiskers for both NH and SC neurons; two-sample Kolmogorov–Smirnov test, $P > 0.05$; Fig. 3b). However, receptive field size in layer II/III neurons was significantly smaller in NH rats compared with SC rats (median receptive field size is two whiskers in NH rats and six whiskers in SC rats; two-sample Kolmogorov–Smirnov test, $P < 0.005$; Fig. 3a). This effect provides a plausible neurophysiological substrate for the contraction of a single whisker’s functional representation reported with optical imaging, but it does not indicate whether the reduction in a whisker representation’s peak amplitude corresponded to a reduction in neuronal firing rate at the centre of the receptive field and/or the surround. The response strength of layer II/III neurons showed a significant suppression to stimulation of the principal whisker (16.13 ± 1.72 versus 22.87 ± 2.3 spikes per second) and adjacent whisker (5.3 ± 0.77 versus 8.4 ± 1.23 spikes per second) in NH compared with SC rats, respectively ($P < 0.05$; Mann–Whitney U -test). In contrast, there was no difference in the principal whisker or adjacent whisker response strength in layer IV between NH and SC rats (see univariate response distributions in Fig. 3c, d).

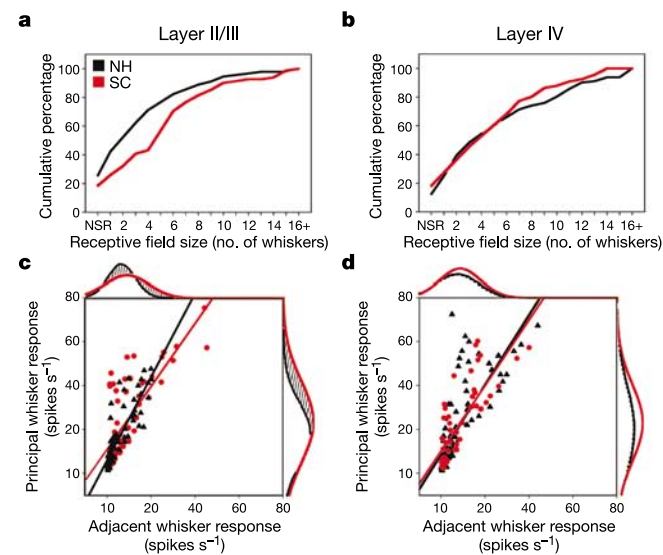


Figure 3 Receptive field plasticity in layer II/III but not IV. Red and black lines represent SC and NH values, respectively. **a, b**, Cumulative percentage graphs represent the distribution of receptive field sizes for neurons recorded in layer II/III (**a**) and IV (**b**). Neurons not significantly responsive to stimulation of any whiskers were identified as NSR. **c, d**, Scatter plots of unit response magnitude to principal and adjacent whisker stimulation for neurons in layer II/III (**c**) and IV (**d**). The principal whisker (right) and adjacent whisker (top) univariate response distributions are shown. Stippled regions indicate significant ($P < 0.05$) differences in the principal-whisker- and adjacent-whisker-evoked response magnitude.

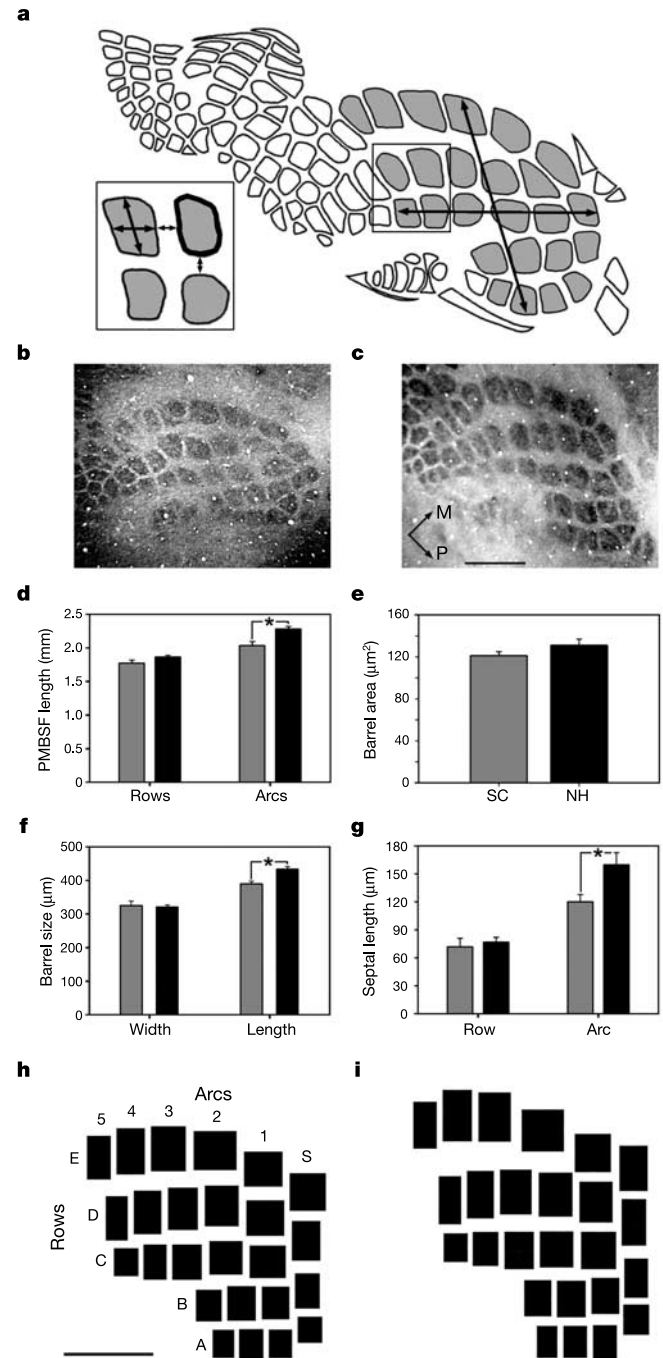


Figure 4 Characterizing morphological plasticity of the layer IV barrel field. **a**, Illustration of the PMBSF (grey) seen in a tangential section through layer IV. Arrows indicate the axis for measuring the length of the PMBSF along arcs (vertical arrow) and rows (horizontal arrow). Inset: axis of measurement for barrel length (vertical arrow), width (horizontal arrow), area (thick line circumscribing the barrel) and the length of septa separating barrels along a row and arc. **b, c**, Cytochrome oxidase reactivity in flattened sections through layer IV of the PMBSF in SC (**b**) and NH (**c**) rats. Arrows indicate medial (M) and posterior (P). Scale bar in **c**, which also applies to **b**, = 1 mm. **d**, PMBSF length across rows and arcs. **e**, Individual barrel area. **f**, Length and width of individual barrels. **g**, Length of septa separating pairs of adjacent barrels along a row or an arc. Asterisks indicate statistically significant differences between NH (black) and SC (grey) groups ($P < 0.05$) using an unpaired t -test. **h, i**, Mean length and width of each individual barrel as well as the mean length of the septa separating each adjacent barrel along a row and arc are drawn to scale to reconstruct the average cytochrome oxidase map for SC (**h**) and NH (**i**) rats. Scale bar = 1 mm.

Interestingly, the suppression was not expressed uniformly across the receptive field. The principal whisker response bias (a ratio of principal whisker/adjacent whisker response strength) was significantly greater in layer II/III neurons from NH versus SC rats (3.8 ± 0.86 versus 2.48 ± 1.0 ; $P < 0.05$, Mann–Whitney U test) but was not different between layer IV neurons. Thus, as illustrated by the difference in the linear regression slopes in Fig. 3c, the response to a stimulus placed in the surround of the receptive field was more strongly suppressed than the response to a stimulus placed at the centre of the receptive field, tantamount to a sharpening of the receptive field rather than a general reduction in response strength. Finally, we compared the spontaneous firing rate (measured immediately before stimulus onset) in SC and NH rats for layer II/III (SC versus NH: 2.96 ± 0.27 versus 3.03 ± 0.27 spikes per second) and layer IV (3.46 ± 0.34 versus 2.98 ± 0.24 spikes per second), but did not find any significant differences between treatment group ($F_{1,347} = 0.73$; $P > 0.05$) or layer ($F_{1,347} = 0.56$; $P > 0.05$). Collectively, these results demonstrate that plasticity is differentially expressed across the receptive field and is specific to evoked, not spontaneous, neuronal responses in the upper cortical layers, and therefore, cannot be attributed to an increased sensitivity to anaesthesia, decreased cortical excitability or a nonspecific adaptation to simple whisker stimuli.

To determine whether the plasticity of the functional whisker map was accompanied by changes in the morphological whisker map, we processed cortical sections from NH and SC rats for cytochrome oxidase reactivity (an activity-dependent enzyme with an expression pattern that co-localizes with the centre of the cytoarchitecturally defined barrels within the PMBSF of the rat¹⁵). Examination of cytochrome oxidase maps from a representative SC (Fig. 4b) and NH rat (Fig. 4c) demonstrates that although the general morphology of the PMBSF is quite similar between groups, the length of the PMBSF in NH rats (2.28 ± 0.04 mm) is modestly, but significantly, longer along the arc axis than in SC rats (2.03 ± 0.07 mm; $t = 3.31$; $P < 0.01$), but was not different along the row axis (SC versus NH: 1.77 ± 0.05 versus 1.86 ± 0.03 mm; $t = 1.69$; $P > 0.05$; Fig. 4d). The constituent barrels were not greater in area (SC versus NH: 121.0 ± 6.23 versus 131.11 ± 3.51 μm^2 ; $t = 1.41$; $P > 0.05$; Fig. 4e) or width (SC versus NH: 325.0 ± 13.1 versus 321.11 ± 6.33 μm ; $t = 2.58$; $P > 0.05$; Fig. 4f), but the length was slightly larger in NH rats (434.44 ± 7.29 μm) compared with SC rats (389.0 ± 9.36 μm ; $t = 3.77$; $P < 0.05$; Fig. 4f). Similarly, the average length of the septa separating barrels along an arc was significantly longer in NH rats (158.89 ± 12.85 μm) compared with SC rats (123.0 ± 8.44 μm ; $t = 2.38$; $P < 0.05$; Fig. 4g), but no differences were observed in the length of the septa along rows (SC versus NH: 72.0 ± 2.91 versus 76.67 ± 5.27 μm ; $t = 0.78$; $P > 0.05$; Fig. 4g).

Further analysis showed that the increase in barrel length was small and homogenous across the PMBSF, but the increase in septal length was spatially restricted and comparatively larger (Fig. 4h, i). For each animal, the PMBSF geometry was reconstructed through measurements of the length and width of all individual barrels, as well as the length of the septa separating each pair of adjacent barrels (Supplementary Fig. S4). Comparison of the averaged PMBSF maps for SC and NH groups demonstrated an increase in barrel length of NH rats in 24 of 25 barrels measured, but by only 10.2% on average (Fig. 4h, i). In contrast, the septal expansion was proportionately much larger and expressed almost exclusively in the anteromedial corner of the PMBSF. In NH rats compared with SC rats, respectively, we observed significant increases in the length of the septa separating barrels D3 and E3 (307 ± 0.03 versus 177 ± 0.02 μm ; $t = 3.42$; $P < 0.01$), D4 and E4 (324 ± 0.06 versus 177 ± 0.03 μm ; $t = 2.8$; $P < 0.05$) and D5 and E5 (302 ± 0.04 versus 182 ± 0.01 μm ; $t = 3.09$; $P < 0.05$). Additionally, we found no difference in the thickness of the cortex (measured in coronal sections through the PMBSF) in NH rats (1.59 ± 0.04 mm) compared to SC rats

(1.63 ± 0.05 mm; unpaired t -test, $t = 0.54$; $P > 0.05$). Further research is needed to determine whether the source of the morphological changes observed in layer IV originate from changes in the thalamocortical connectivity patterns or from changes that originate within layer IV itself and are thus independent of the thalamocortical input.

We found that individual whisker representations contract to nearly half of their original area after one month in the NH. The magnitude of this effect is surprisingly large given the age of the animals and the absence of an imbalance of sensory inputs at the periphery (for example, whisker trimming or follicle lesion) which would strongly drive competitive plasticity mechanisms. The functional contraction and response suppression that was reported after prolonged exposure to the NH might have been consolidated from the rapid attenuation of sensory-evoked responses in the barrel cortex, known to occur during bouts of active whisking in awake rats^{16,17}. In support of this finding, it has recently been shown that the peak amplitude and spatial spread of whisker-evoked activity in the barrel cortex are strongly reduced and receptive fields are sharpened during acute stimulation of the reticular formation, a technique that imitates the physiological conditions of natural arousal^{17,18}. Furthermore, increasing sensory activity through early exposure to enriched environments^{19,20} or by continuous whisker stimulation²¹, increases response selectivity in the cortex, perhaps through upregulating inhibitory intracortical synapses²² or increasing levels of neurotrophins such as brain-derived neurotrophic factor²³. The laminar specificity for these changes reinforces the concept that supragranular layers of the barrel cortex remain plastic for a longer period than the granular layer^{5,7,24}, and that these changes are probably mediated through plasticity of intracortical circuits^{25,26}. In our previous study, we reported that a few minutes per week of natural whisker use outside the home cage induced a contraction of whisker representations and a reduction of their peak amplitude in the barrel cortex of adult rats with partially removed whisker arrays, but had no effect on the area of a single whisker's representation in rats with fully intact whisker arrays³. Our data demonstrate that this type of plasticity can also occur in layer II/III of non-deprived adult rats that engage in natural behaviours, suggesting that smaller, more metabolically efficient whisker representations and smaller, sharper receptive fields (an apparent refinement of cortical maps) are a characteristic feature of cortical organization in rats that are allowed sufficient opportunity to express innate behaviours. □

Methods

Housing conditions

Male Sprague–Dawley rats were reared in standard cages until they were at least 90 days old. Rats were then randomly assigned to live in NH or modified SC conditions. The NH was created from a circular steel tank, 2 m in diameter and 1 m deep, filled to approximately 70% capacity with packed, sterile topsoil. An extensive labyrinth of tunnels containing objects with a wide variety of textures and shapes was built on top of the packed soil. Eight to ten rats were simultaneously placed in the NH and remained there continuously for 28 to 42 days. Rats assigned to the SC were housed in standard individual cages ($33 \times 22 \times 15$ cm) for 28 to 39 days. Standard cages were filled with packed soil from the NH and placed side-by-side less than a meter away from the NH to make the level of non-somatosensory stimulus modalities more similar to NH rats.

Surgical procedures

Rats were anaesthetized with sodium pentobarbital (50 mg kg^{-1} followed by supplements as needed, approximately 15 mg kg^{-1}). In optical imaging experiments, the skull overlying the left barrel cortex was thinned and enclosed with a petroleum jelly well, filled with saline to create a transparent, non-invasive cortical window. In electrophysiological recording experiments, a craniotomy was performed over the left barrel cortex and the dura was reflected.

Optical imaging

A detailed description of the chronic ISI procedure has been described previously²⁷. Chronic high-resolution images were obtained from adult male rats (375 – 600 g) before and after assignment to NH ($n = 13$) or SC ($n = 8$) housing conditions. Images were obtained under stabilized 630 nm light with a slow-scan CCD camera (Quantix, Roper

Scientific), defocused 500 μm beneath the cortical surface. Sixty-four single trials were summed and divided into eleven 500 ms frames for image visualization and analysis. After 1 s of prestimulus data acquisition, an individual whisker was displaced 1.9° rostrocaudally at 5 Hz for 1 s.

Electrophysiology

Extracellular recordings of 449 single and multiple units were obtained from seven NH and seven SC rats. In some cases ($n = 100$ units; two rats from each group), layer II/III recordings were obtained only to verify correspondence with optical imaging data (see Supplementary Fig. S2). In all other cases ($n = 349$), individual whisker representations were visualized immediately before electrophysiological recordings with ISI to guide electrode placement into specific regions of the barrel field (Supplementary Fig. S3). Neural activity was filtered, amplified and sorted simultaneously from an array of eight low impedance (1–2 m Ω) tungsten microelectrodes (Microprobe) using a multi-channel acquisition and online spike sorting system (Alpha Omega). Recordings were obtained from 7–8 locations in layer II/III and layer IV in each rat. Often, more than one single unit waveform was isolated from a single electrode. Electrode depth was matched to cortical laminae by post-mortem histology.

Cytochrome oxidase histochemistry

A separate set of 19 rats (NH, $n = 9$; SC, $n = 10$) were perfused intracardially and the left hemisphere was sectioned tangentially. In some cases (NH, $n = 8$; SC, $n = 7$), the right hemisphere was also removed and sectioned in the coronal plane. All sections were stained for cytochrome oxidase reactivity using a standard rat protocol¹⁵.

Analysis of optical imaging data

A detailed account of areal extent analysis procedures can be found elsewhere²⁸. Briefly, an intratrial division analysis designed to focus on the initial decrease in deoxyhaemoglobin levels was applied to each square 34 μm pixel, within the 191 \times 144 pixel image. Ratio images were created by dividing poststimulus intrinsic signal activity (collected 0.5 s up to 1.5 s poststimulus onset) by prestimulus intrinsic signal activity (collected during the 500 ms immediately preceding stimulus onset). Ratio images were gaussian filtered (half width = 5) and the areal extent of each whisker's functional representation was quantified at seven threshold levels above the median prestimulus activity level (from 1.5×10^{-4} to 3.0×10^{-4} , in 0.25×10^{-4} increments). In all but four rats, it was possible to image the representation of several single whiskers (whiskers C1 and C2 in 14 rats; C1, C2 and B2 in 3 rats). Whiskers were stimulated individually in all cases. Areal extent values obtained for each whisker were averaged so that each rat contributed a single value for all measures. All values are expressed as mean \pm standard error. The peak of a functional whisker representation was defined as the single pixel with the greatest post-/pre-ratio value. Peak amplitude is calculated as the peak intrinsic signal response minus median prestimulus intrinsic signal response. It has recently been demonstrated that the peak of the functional whisker representation, defined in this manner, directly overlies the centre of the corresponding layer IV barrel²⁹.

Analysis of electrophysiological recordings

Receptive field and response magnitude measurements were derived from single and multiunit responses to stimulation of 25 whiskers on the contralateral face (AB–A3, BC–B3, CD–C5, DE–D5, E1–E5) independently presented in a pseudorandom order. Whiskers were displaced 1.9° rostrocaudally at 5 Hz for 1 s with a glass capillary tube, attached to a fast piezoelectric biomorph wafer for 40 stimulus repetitions. Receptive field size was calculated by counting the number of whiskers that evoked a response, exceeding a $P < 0.01$ significance threshold (determined by a Poisson probability function applied to spontaneous activity, during the 500 ms preceding stimulus onset) during a 50 ms period, beginning 7 ms after stimulus onset³⁰. Mean spontaneous firing rate was defined as the average firing rate during a 300 ms period, beginning 350 ms before stimulus onset. The magnitude of the stimulus-evoked response was calculated by subtracting the mean spontaneous firing rate from activity occurring in a 50 ms period, beginning 7 ms after stimulus onset. Measurements of evoked response magnitude were only calculated from units that had a receptive field size of at least one whisker. The principal whisker was defined in these units as the whisker that evoked the highest magnitude response. Adjacent whisker response strength was obtained from the average of all adjacent whiskers along the row and arc.

Morphometric analysis of cytochrome oxidase reactivity

Cytochrome oxidase reactivity was measured in coronal and tangential sections. A digital image of each section was obtained at $\times 4$ and $\times 20$ magnification. Cortical thickness was defined as the average distance between the white matter and cortical surface in sections drawn from anterior, central and posterior regions of the barrel cortex. The PMBSF was defined in tangential sections as the region of the barrel cortex containing barrels AB–A3, BC–B3, CD–C5, DE–D5, E1–E5 (Fig. 4a). Three categories of measurements were obtained from tangential sections in NH ($n = 9$) and SC rats ($n = 10$): (1) the average length of the entire PMBSF was measured across arcs (5, 4, 3, 2, 1 and straddler) and rows (A, B, C, D and E); (2) the width, length and area of all 25 barrels; (3) the length of the septa separating all pairs of adjacent barrels. All measurements were performed with measurement tools in Photoshop (Adobe Systems).

Data collection could not be performed blind due to changes in the appearance of the NH rats, but analysis of the cytochrome oxidase maps and electrophysiological data were performed blind to treatment group.

Received 5 December 2003; accepted 2 March 2004; doi:10.1038/nature02469.

1. Buonomano, D. V. & Merzenich, M. M. Cortical plasticity: from synapses to maps. *Annu. Rev. Neurosci.* **21**, 149–186 (1998).
2. Kaas, J. H. in *The New Cognitive Neurosciences* (ed. Gazzaniga, M. S.) 223–236 (MIT Press, Cambridge, Massachusetts, 2000).
3. Polley, D. B., Chen-Bee, C. H. & Frostig, R. D. Two directions of plasticity in the sensory-deprived adult cortex. *Neuron* **24**, 623–637 (1999).
4. Simons, D. J. & Land, P. W. Early experience of tactile stimulation influences organization of somatic sensory cortex. *Nature* **326**, 694–697 (1987).
5. Fox, K. A critical period for experience-dependent synaptic plasticity in rat barrel cortex. *J. Neurosci.* **12**, 1826–1838 (1992).
6. Diamond, M. E., Armstrong-James, M. & Ebner, F. F. Experience-dependent plasticity in adult rat barrel cortex. *Proc. Natl Acad. Sci. USA* **90**, 2082–2086 (1993).
7. Glazewski, S. & Fox, K. Time course of experience-dependent synaptic potentiation and depression in barrel cortex of adolescent rats. *J. Neurophysiol.* **75**, 1714–1729 (1996).
8. Kossut, M., Hand, P. J., Greenberg, J. & Hand, C. L. Single vibrissal cortical column in SI cortex of rat and its alterations in neonatal and adult vibrissa-deafferented animals: a quantitative 2DG study. *J. Neurophysiol.* **60**, 829–852 (1988).
9. Woolsey, T. A. & Van der Loos, H. The structural organization of layer IV in the somatosensory region (SI) of mouse cerebral cortex. The description of a cortical field composed of discrete cytoarchitectonic units. *Brain Res.* **17**, 205–242 (1970).
10. Van der Loos, H. & Woolsey, T. A. Somatosensory cortex: structural alterations following early injury to sense organs. *Science* **179**, 395–398 (1973).
11. Jeannonod, D., Rice, F. L. & Van der Loos, H. Mouse somatosensory cortex: alterations in the barrel field following receptor injury at different early postnatal ages. *Neuroscience* **6**, 1503–1535 (1981).
12. Bennett, E. L., Diamond, M. C., Krech, D. & Rosenzweig, M. R. Chemical and anatomical plasticity of brain. *Science* **146**, 610–619 (1964).
13. Uylings, H. B., Kuypers, K., Diamond, M. C. & Veltman, W. A. Effects of differential environments on plasticity of dendrites of cortical pyramidal neurons in adult rats. *Exp. Neurol.* **62**, 658–677 (1978).
14. Green, E. J., Greenough, W. T. & Schlumpf, B. E. Effects of complex or isolated environments on cortical dendrites of middle-aged rats. *Brain Res.* **264**, 233–240 (1983).
15. Land, P. W. & Simons, D. J. Cytochrome oxidase staining in the rat Sml barrel cortex. *J. Comp. Neurol.* **238**, 225–235 (1985).
16. Fanselow, E. E. & Nicolelis, M. A. Behavioural modulation of tactile responses in the rat somatosensory system. *J. Neurosci.* **19**, 7603–7616 (1999).
17. Castro-Alamancos, M. A. Role of thalamocortical sensory suppression during arousal: focusing sensory inputs in neocortex. *J. Neurosci.* **22**, 9651–9655 (2002).
18. Castro-Alamancos, M. A. & Oldford, E. Cortical sensory suppression during arousal is due to the activity-dependent depression of thalamocortical synapses. *J. Physiol. (Lond.)* **541**, 319–331 (2002).
19. Beaulieu, C. & Cynader, M. Effect of the richness of the environment on neurons in cat visual cortex. I. Receptive field properties. *Brain Res. Dev. Brain Res.* **53**, 71–81 (1990).
20. Coq, J. O. & Kerri, C. Environmental enrichment alters organizational features of the forepaw representation in the primary somatosensory cortex of adult rats. *Exp. Brain Res.* **121**, 191–204 (1998).
21. Welker, E., Rao, S. B., Dorfl, J., Melzer, P. & van der Loos, H. Plasticity in the barrel cortex of the adult mouse: effects of chronic stimulation upon deoxyglucose uptake in the behaving animal. *J. Neurosci.* **12**, 153–170 (1992).
22. Knott, G. W., Quairiaux, C., Genoud, C. & Welker, E. Formation of dendritic spines with GABAergic synapses induced by whisker stimulation in adult mice. *Neuron* **34**, 265–273 (2002).
23. Prakash, N., Cohen-Cory, S. & Frostig, R. D. Rapid and opposite effects of BDNF and NGF on the functional organization of the adult cortex *in vivo*. *Nature* **381**, 702–706 (1996).
24. Stern, E. A., Maravall, M. & Svoboda, K. Rapid development and plasticity of layer 2/3 maps in rat barrel cortex *in vivo*. *Neuron* **31**, 305–315 (2001).
25. Zarzecki, P. *et al.* Synaptic mechanisms of cortical representational plasticity: somatosensory and corticocortical EPSPs in reorganized raccoon SI cortex. *J. Neurophysiol.* **69**, 1422–1432 (1993).
26. Fox, K. The cortical component of experience-dependent synaptic plasticity in the rat barrel cortex. *J. Neurosci.* **14**, 7665–7679 (1994).
27. Frostig, R. D., Chen-Bee, C. H. & Polley, D. B. in *In Vivo Optical Imaging of Brain Function* (ed. Frostig, R. D.) 21–42 (CRC Press, Boca Raton, 2002).
28. Chen-Bee, C. H. *et al.* Visualizing and quantifying evoked cortical activity assessed with intrinsic signal imaging. *J. Neurosci. Methods* **97**, 157–173 (2000).
29. Brett-Green, B., Chen-Bee, C. H. & Frostig, R. D. Comparing the functional representations of central and border whiskers in rat primary somatosensory cortex. *J. Neurosci.* **21**, 9944–9954 (2001).
30. Abeles, M. Quantification, smoothing, and confidence limits for single-units' histograms. *J. Neurosci. Methods* **5**, 317–325 (1982).

Supplementary Information accompanies the paper on www.nature.com/nature.

Acknowledgements We would like to thank L. Sininger, J. Rickert and C. Chen-Bee for assistance with data analysis and maintaining the naturalistic habitat, and D. Simmons and P. Yahr for their histology expertise. We would like to thank S. Bao, T. Carew, M. Leon, C. Moore, F. Strata and N. Weinberger for comments on the manuscript and M. Leon for suggestions on the use of a NH. This work was supported by National Institute of Health-National Institute of Neurological Disorders and Stroke grants to R.D.F.

Competing interests statement The authors declare that they have no competing financial interests.

Correspondence and requests for materials should be addressed to D.P. (dpolley@phy.ucsf.edu).